View metadata, citation and similar papers at core.ac.uk
brought to you by CORE
provided by Carolina Digital Repository

The EMBO Journal (2012) 31, 1494–1505 | © 2012 European Molecular Biology Organization | All rights reserved 0261-4189/12
www.embojournal.org
THE EMBO JOURNAL

Myeloid translocation gene 16 is required for maintenance of haematopoietic stem cell quiescence

Melissa A Fischer[1], Isabel Moreno-Miralles[1,2], Aubrey Hunt[1], Brenda J Chyla[1,4] and Scott W Hiebert[1,3,*]

[1]Department of Biochemistry, Vanderbilt University School of Medicine, Nashville, TN, USA, [2]McAllister Heart Institute, University of North Carolina, Chapel Hill, NC, USA and [3]Vanderbilt-Ingram Cancer Center, Vanderbilt University School of Medicine, Nashville, TN, USA

The t(8;21) and t(16;21) that are associated with acute myeloid leukaemia disrupt two closely related genes termed *Myeloid Translocation Genes 8* (*MTG8*) and *16* (*MTG16*), respectively. Many of the transcription factors that recruit Mtg16 regulate haematopoietic stem and progenitor cell functions and are required to maintain stem cell self-renewal potential. Accordingly, we found that *Mtg16*-null bone marrow (BM) failed in BM transplant assays. Moreover, when removed from the animal, *Mtg16*-deficient stem cells continued to show defects in stem cell self-renewal assays, suggesting a requirement for Mtg16 in this process. Gene expression analysis indicated that *Mtg16* was required to suppress the expression of several key cell-cycle regulators including *E2F2*, and chromatin immunoprecipitation assays detected Mtg16 near an E2A binding site within the first intron of *E2F2*. BrdU incorporation assays indicated that in the absence of *Mtg16* more long-term stem cells were in the S phase, even after competitive BM transplantation where normal stem and progenitor cells are present, suggesting that Mtg16 plays a role in the maintenance of stem cell quiescence.

The EMBO Journal (2012) **31,** 1494–1505. doi:10.1038/emboj.2011.500; Published online 20 January 2012
Subject Categories: development; differentiation & death
Keywords: CBFA2T3; haematopoietic stem cells; myeloid leukaemia; transcription

Introduction

Non-random, somatically acquired, chromosomal translocations are commonly associated with the development of acute leukaemia and affect genes that control cell proliferation, differentiation, survival, and lineage decisions that affect stem cell self-renewal and progenitor cell differentiation (Hope *et al*, 2003). While translocations can cause the over-expression of dominantly acting oncogenes such as *BCL2* or *c-MYC* (Dalla-Favera *et al*, 1982; Graninger *et al*, 1987), the majority of the fusion proteins that are created in the myeloid lineage create weak oncogenes that do not have a single dominant phenotype. As such, the genes that are disrupted by these translocations have been extensively studied in order to understand the function of the translocation fusion proteins. The t(8;21) and t(16;21) target two closely related Myeloid Translocation Gene (MTG) family members, *MTG8* (also known as *RUNX1T1* or *ETO*) and *MTG16* (also known as *CBFA2T3* or *ETO2*), respectively. The t(8;21) is associated with 12–15% of *de-novo* acute myeloid leukaemia (AML) cases, while the t(16;21) is more rare and associated with therapy-related AML (Miyoshi *et al*, 1991; Erickson *et al*, 1992; Gamou *et al*, 1998; Davis *et al*, 1999). Both of these translocations create fusion proteins containing the DNA binding domain of RUNX1 (formerly called AML1) fused to nearly full-length of MTG8 or MTG16 (Miyoshi *et al*, 1991, 1993; Erickson *et al*, 1992; Gamou *et al*, 1998).

These fusion proteins have the capacity to repress genes containing a RUNX1 DNA binding site such as $p14^{ARF}$ (*Cdkn2a isoform4*), *Neurofibromatosis-1* (*Nf-1*), *PU.1* (*Spi1*), and *C/EBPα* (*Cebpa*) (Pabst *et al*, 2001; Linggi *et al*, 2002; Vangala *et al*, 2003; Yang *et al*, 2005). While repression of tumour suppressor genes is an attractive hypothesis for how these fusion proteins trigger leukaemia, these translocations also disrupt one allele of *RUNX1* and either *MTG8* or *MTG16*, suggesting that haploinsufficiency or impairment of *RUNX1* or *MTG8/MTG16* may also contribute to leukaemogenesis. For *RUNX1* and its closely related family member RUNX3, mouse models with deletions of these genes have supported this hypothesis (Song *et al*, 1999; Li *et al*, 2002; Silva *et al*, 2003). For the MTG family, possible inactivating mutations have been identified in *MTG8* in colon, lung, and breast cancer (including a frame shift mutation), whereas *MTG16* mutations were found in ovarian cancer (Wood *et al*, 2007; Kan *et al*, 2010). MTG family members also have the ability to form oligomers, and the fusion proteins associated with leukaemia bind to the wild-type MTGs that remain (Kitabayashi *et al*, 1998; Zhang *et al*, 2004; Liu *et al*, 2006). These data suggest that loss of function of MTG proteins could contribute to leukaemogenesis; yet, the mechanism by which this might occur remains obscure.

The ability of the t(8;21) fusion protein to repress transcription suggested that the MTG family members act as transcriptional co-repressors. This repression is mediated by the recruitment of the mSin3 and N-CoR/SMRT co-repressors and class I histone deacetylases (Gelmetti *et al*, 1998; Lutterbach *et al*, 1998; Wang *et al*, 1998; Amann *et al*, 2001; Hildebrand *et al*, 2001). As expected for transcriptional co-repressors, MTG family members are recruited by many site-specific DNA binding proteins, including Gfi1, Gfi1B, TAL1/SCL, the 'E proteins' E2A and HEB, BTB-POZ domain factors BCL6 and PLZF, and mediators of Wnt and Notch

*Corresponding author. Department of Biochemistry, Vanderbilt University School of Medicine, 512 Preston Research Building, 2220 Pierce Avenue, Nashville, TN 37232, USA. Tel.: +1 615 936 3582; Fax: +1 615 936 1790; E-mail: scott.hiebert@vanderbilt.edu
[4]Present address: Abbott Laboratories, Abbott Park, IL, USA

Received: 18 July 2011; accepted: 16 December 2011; published online: 20 January 2012

©2012 European Molecular Biology Organization

signalling (TCF4 and CSL) (Melnick *et al*, 2000; McGhee *et al*, 2003; Chevallier *et al*, 2004; Zhang *et al*, 2004; Schuh *et al*, 2005; Goardon *et al*, 2006; Moore *et al*, 2008; Salat *et al*, 2008; Engel *et al*, 2010; Soler *et al*, 2010). E proteins may play key roles as the association is robust and a point mutant of Mtg16/Eto2 lacking the ability to regulate E2A or HEB failed to complement *Mtg16*$^{-/-}$-associated defects in T-cell differentiation (Hunt *et al*, 2011). Thus, MTG family members play a pivotal function during haematopoiesis to link DNA binding transcription factors to chromatin modifying enzymes to influence gene expression.

The balance between haematopoietic stem cell (HSC) differentiation and self-renewal must be maintained to ensure homeostasis, long-term stem cell viability, and suppress cancer formation (Santaguida *et al*, 2009). Thus, the discovery of factors that control these processes in HSCs is important in terms of tumourigenesis and for their use in clinical applications such as haematopoietic cell transplantation. In addition, understanding the role of regulatory factors in HSC function can be applied to other organ systems (Shizuru *et al*, 2005). Interestingly, the engineered inactivation of many transcription factors that recruit MTG family members identified them as key regulators of stem cell functions and lineage allocation in mice. In several instances, these phenotypes were related to inappropriate cycling of the lineage-negative, Sca1$^+$, c-Kit$^+$ (LSK) stem/progenitor cells (e.g., Gfi1, E2A), which caused depletion of stem cell pools or non-competitive long-term stem cells (Hock *et al*, 2004; Zeng *et al*, 2004; Semerad *et al*, 2009). These data suggest that MTG family members might contribute to stem cell functions.

Mtg16 is the dominant MTG family member expressed in haematopoietic stem and early progenitor cells and microarray profiling of normal and leukaemic stem cells suggests that *Mtg16* is expressed in these cells (Lindberg *et al*, 2005; Deneault *et al*, 2009). Moreover, MTG family members appear to act through E proteins that are critical for stem cell homeostasis. Here, we demonstrate that inactivation of *Mtg16* caused a reduction in HSC pools that could be traced to the hyperactive cycling of stem cells (lineage-negative, Sca1$^+$/c-Kit$^+$, LSK cells, LSK/Flt3$^-$, and LSK/CD150$^+$/CD48$^-$). This uncontrolled cycling led to stem cell exhaustion after serial competitive bone marrow (BM) transplantation. The increased cycling was associated with the inappropriate expression of *E2F2*, *Cyclin D1* (*Ccnd1*), and *N-Myc* (*Mycn*) and was evident even after competitive BM transplantation, suggesting a cell intrinsic defect. Chromatin immunoprecipitation (ChIP) directly linked Mtg16/Eto2 to an enhancer in the first intron of *E2F2*, which is a putative target for regulation by E proteins. Thus, Mtg16 plays a key role in suppressing the entry of HSCs into the cell cycle.

Results

Defects in Mtg16-null HSCs

Mtg16$^{-/-}$ mice show only modest haematopoietic defects, but when challenged they lacked the ability to respond to erythropoietic stress (Chyla *et al*, 2008). These results, along with the linkage of MTG family members to Wnt and Notch signalling, prompted us to carefully examine the haematopoietic stem and progenitor cell compartments in *Mtg16*$^{-/-}$ mice. We used flow cytometry to identify lineage-negative, Sca1$^+$, c-Kit$^+$ (LSK) cells, which represent stem and early progenitor cells. These cells were reduced by roughly two-fold in *Mtg16*$^{-/-}$ mice and when these cells were further divided based on Flt3 expression to focus in on the stem cell population, the LSK/Flt3$^-$ cells were also reduced by nearly two-fold (Figure 1A–C). To confirm the reduction in the stem cell population, we further fractionated the LSK/Flt3$^-$ cells with the signalling lymphocyte attractant molecule (SLAM) markers CD150 and CD48, which greatly enriches for long-term repopulating HSCs (LT-HSC) (Kiel *et al*, 2005). The LSK/Flt3$^-$/CD150$^+$/CD48$^-$ fraction of cells (LT-HSC) was also reduced by slightly >2-fold in the *Mtg16*$^{-/-}$ mice (Figure 1D).

Next, we used BM transplantation assays to assess stem cell functions. While injection of only 200 000 wild-type cells were sufficient to provide radioprotection and yielded 100% survival, injection of 200 000 *Mtg16*-deficient cells failed to reconstitute the marrow with all mice succumbing within 30 days. Injection of one million cells only extended the survival to a maximum of 52 days, suggesting that the stem cells were defective in repopulating the marrow (Figure 2A). However, the impaired erythroid progenitor cell function observed previously could also contribute to this phenotype. Therefore, we performed competitive BM transplants to assess stem cell function in the context of wild-type progenitor cells using 10% wild-type (CD45.1$^+$) cells to provide radioprotection along with 90% *Mtg16*$^{-/-}$ (CD45.2$^+$) BM cells. Given that there were only about 25% of the normal complement of stem cells (Figure 1), using a 9:1 ratio of null to wild-type cells equates to using roughly two-fold more null stem cells than wild type. Within 7 weeks of transplant there were already substantial reductions in the number of *Mtg16*$^{-/-}$ cells in the peripheral blood with only 25–30% CD45.2$^+$ cells present (Figure 2B). By 13 weeks post transplant, when the peripheral blood cells are derived from the long-term stem cells, the percentage of CD45.2$^+$ cells had dropped to <20%. These cells continued to erode over time falling to nearly 10% after 1 year while control CD45.2$^+$ cells maintained a level of at least 90% (Figure 2B).

Although the analysis of peripheral blood suggested dramatic defects in *Mtg16*$^{-/-}$ stem cells, excluding erythrocytes, the peripheral blood is mostly composed of B and T cells. Given that *Mtg16*$^{-/-}$ mice have decreased numbers of B cells under homeostasis (Chyla *et al*, 2008) and *Mtg16* is required for the differentiation of T cells (Hunt *et al*, 2011), we used flow cytometry analysis to examine the BM 12 weeks after competitive transplantation. We found a 2–3-fold reduction in CD45.2$^+$ cells in the total BM (Figure 2C and D), whereas only half this number of cells (about 20%) made it into the peripheral blood (Figure 2B). A further breakdown of the contribution of CD45.2$^+$ cells in the BM showed loss of lymphoid cells and a skewing of the *Mtg16*$^{-/-}$ cells towards the myeloid lineage with over 80% of the *Mtg16*$^{-/-}$ cells being Gr1$^+$ and/or Mac1$^+$ (Supplementary Figure S1A and B), which is an exaggeration of the phenotype observed at homeostasis (Chyla *et al*, 2008).

We also examined the LSK and LSK/Flt3$^-$ cells in the BM to determine the number of CD45.2$^+$ cells that remained at 12 weeks post transplant (Figure 2D; Supplementary Figure S2). There was a 2.8-fold reduction in CD45.2$^+$ LSK cells, and a 3-fold reduction in CD45.2$^+$ LSK/Flt3$^-$ stem cells that derived from the *Mtg16*$^{-/-}$ mice (Figure 2D; Supplementary Figure S2 for FACS plots). Given that we started with roughly two times more stem cells by using a 9:1 ratio of null to wild-type cells

©2012 European Molecular Biology Organization

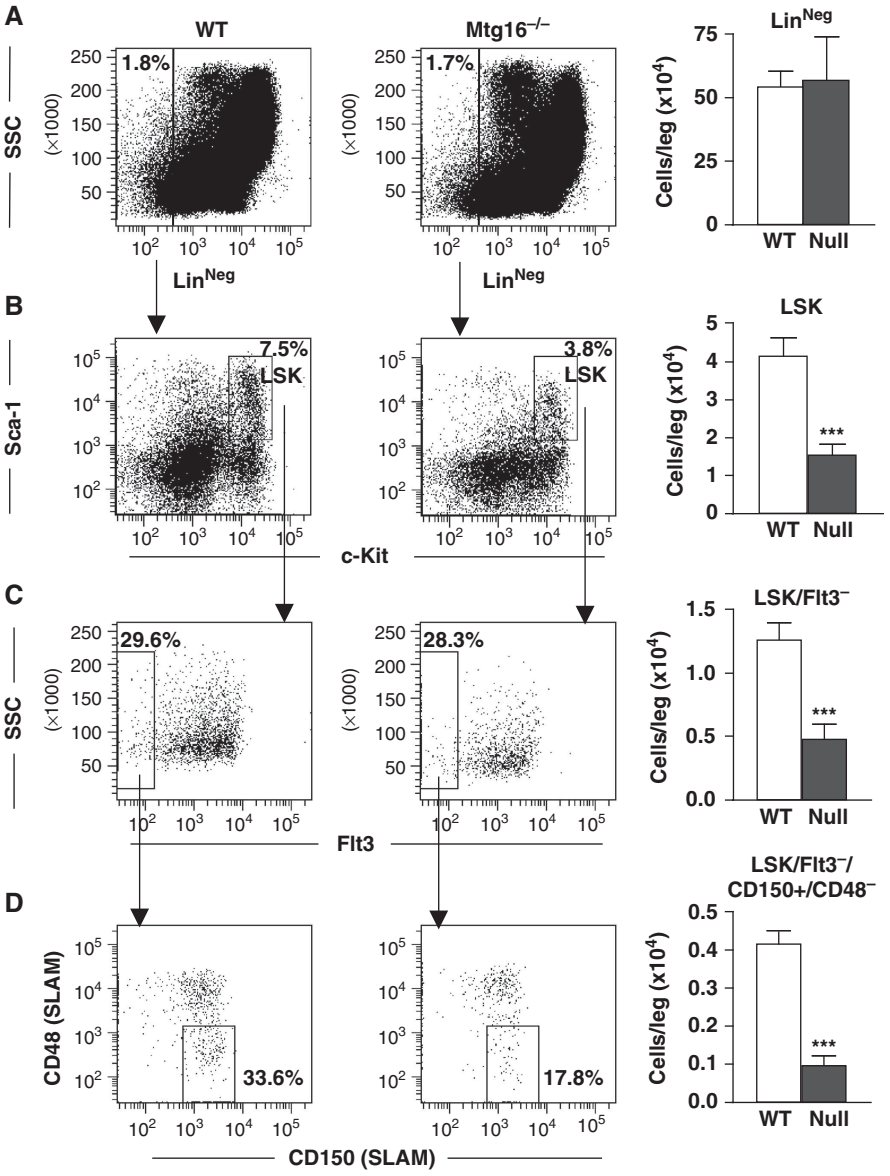

Figure 1 Inactivation of *Mtg16* decreases HSC numbers. Quantification of flow cytometry of whole bone marrow cells. Lineage-negative cells were gated (**A**) and further analysed using anti-Sca-1 and anti-c-Kit (**B**; LSK). The LSK cells were further fractionated using anti-Flt3 to obtain the LSK/Flt3$^-$ (**C**), which was further divided using anti-CD150/anti-CD48 to identify the LSK/Flt3$^-$/CD150$^+$/CD48$^-$ populations (**D**). Quantification of each of these populations is calculated for the number of cells per leg (femur + tibia) and is shown to the right of each dot plot (wild type $n = 5$, empty bars; *Mtg16*-null $n = 5$, full bars). Data are expressed as mean ± the standard error of the mean (s.e.m.). An unpaired two-tailed *t*-test indicated that the changes observed in the number of cells were significant (***$P \leqslant 0.0001$).

(starting material contains 25% of the normal complement of LSK/Flt3$^-$/CD150$^+$/CD48$^-$ cells, Figure 1, multiplied by a 9:1 ratio), there was an overall 5–6-fold defect in stem cell activity. Next, we performed a secondary transplant to further examine *Mtg16*$^{-/-}$ stem cell functions. Six weeks after transplanting irradiated recipient mice with BM from primary transplants that contained from 25 to 45% CD45.2$^+$ BM (*Mtg16*$^{-/-}$), there was a dramatic loss of *Mtg16*$^{-/-}$ cells in the peripheral blood and flow cytometry analysis of the BM of these mice indicated a near complete loss of *Mtg16*$^{-/-}$ LSK and LSK/Flt3$^-$ cells (Figure 3; Supplementary Figure S3 for FACS plots). By contrast, control mice contained 80–90% CD45.2$^+$ cells in the BM (Figure 3). Thus, *Mtg16* is required to maintain stem cells, even when normal progenitor cells are present, suggesting a stem cell intrinsic defect.

To ensure that the observed stem cell defects were not due to contributions from the BM stroma, we assessed the expression of Mtg16 in adult BM stromal fibroblasts as compared with murine erythroleukaemia (MEL) cells and murine embryonic fibroblasts (MEFs). Quantitative real-time PCR showed that Mtg16 was expressed at much lower levels in adult BM stromal cells or MEFs, as compared with its closely related family member, Mtgr1 (CBFA2T2), which was robustly expressed in both cell types, whereas Mtg8/ETO (RUNX1T1) was robustly expressed in MEFs but not in adult BM fibroblasts (Supplementary Figure S4). The low levels of Mtg16 mRNA were confirmed by a concordant lack of readily detectable Mtg16 protein in the BM stromal cells (data not shown). In addition, we did not observe an increase in stem cell numbers in the peripheral blood of *Mtg16*$^{-/-}$ mice,

 ©2012 European Molecular Biology Organization

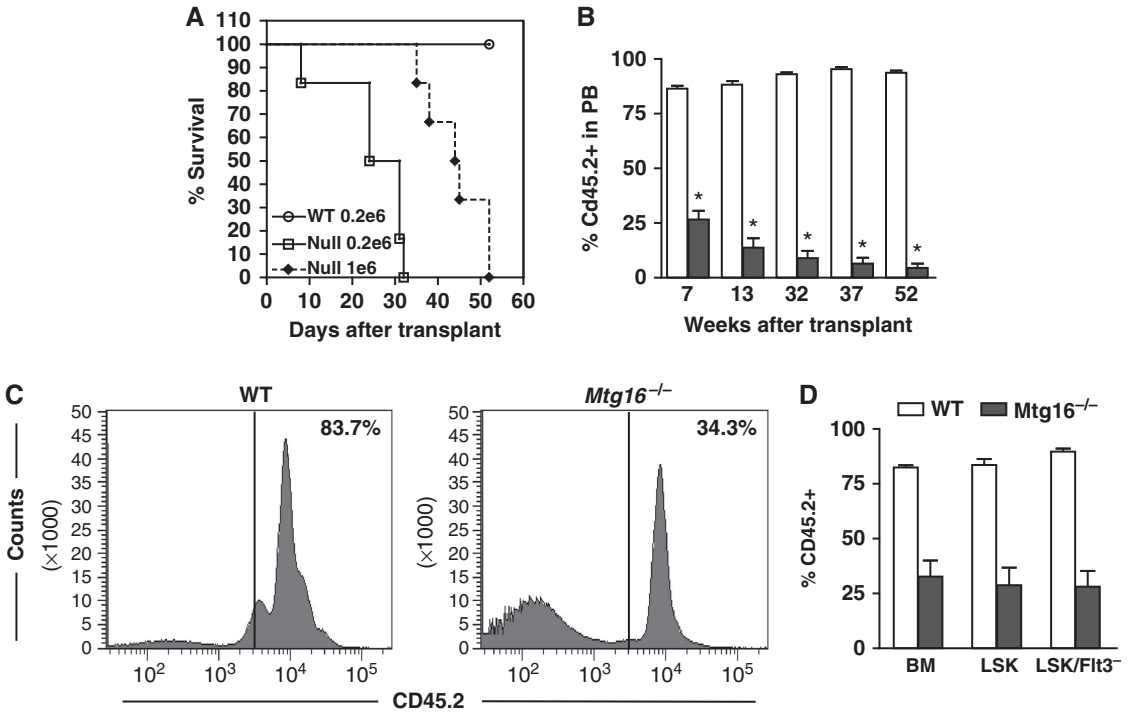

Figure 2 Inactivation of *Mtg16* disrupts HSC functions. (**A**) Survival curves of a representative transplant experiment using 200 000 wild-type bone marrow (BM) cells (open circles), 200 000 *Mtg16*-null BM cells (open boxes), or 1 000 000 *Mtg16*-null bone marrow cells (filled diamonds). (**B**) Competitive repopulation assay where 90% control (empty bars) or *Mtg16*-null (filled bars) CD45.2$^+$ BM cells were co-injected with 10% wild-type CD45.1$^+$ cells. The contribution of each population to long-term reconstitution of the BM was assessed by flow cytometry using anti-CD45.1 and anti-CD45.2 to enumerate cells in the peripheral blood. Data are expressed as mean ± s.e.m. at different times after transplantation. An unpaired two-tailed *t*-test indicated these differences (marked by an *) were statistically significant at all time points after transplantation ($P<0.0001$; $n=5$). (**C**) Flow cytometry analysis of whole BM to determine the percentage of CD45.2 that had repopulated the bone marrow 12 weeks after a competitive repopulation assay. A representative plot from an experiment performed in triplicate that is consistent with other biological replicates is shown. (**D**) Graphical representation of the quantification of CD45.2 cells residing in the BM and LSK or LSK/Flt3$^-$ compartments 12 weeks after competitive BM transplantation.

suggesting that the null stem cells were maintained within the BM niche (data not shown).

Mtg16$^{-/-}$ *cells home to the BM*

To ensure that this defect was not simply due to a failure of the stem cells to home to the marrow, we labelled BM cells *ex vivo* with the vital dye carboxyfluorescein succinimidyl ester (CFSE) before injecting these cells into the tail vein of mice. Sixteen hours later, the BM of these mice was analysed by flow cytometry and the number of cells positive for CFSE was quantified (Figure 4A). A similar number of null cells as compared with wild-type controls were found in the BM. Given that the CFSE experiment assessed whole BM, we further examined the homing of stem and progenitor cells by performing methylcellulose colony formation assays 16 h after BM transplantation and calculating the percentage of stem/progenitor cells that correctly homed to the BM (Figure 4B). The small changes observed were within the statistical error, indicating that immature *Mtg16*$^{-/-}$ cells homed correctly to the marrow (note that irradiated controls yielded only 5–6 colonies compared with 50–75 colonies from injected mice, and this background level was removed in the calculation of the percent of homing).

Mtg16 deficiency affects stem cell self-renewal

The haematopoietic defects found in the LSK/Flt3$^-$ and LSK/CD48$^-$/CD150$^+$ stem cell compartments (Figure 1) and identified in BM transplantation assays, suggested that Mtg16 was required for stem cell self-renewal (Figure 3). To further define the defect, we used *in-vitro* analyses of stem cell functions. First, we serially cultured BM cells in methylcellulose. Stem cells from control mice were able to form colonies through three consecutive rounds of culture in methylcellulose containing IL6, stem cell factor (SCF), erythropoietin, and IL3, but yielded only about 15% of the number of colonies after the fourth culture (Figure 5A). By contrast, *Mtg16*-null cells displayed a four-fold reduction in replating ability after the second round of culture (Figure 5A) and were essentially exhausted by the fourth culture. We extended these results by testing the function of *Mtg16*-null stem cells in a long-term culture-initiating cell (LTC-IC) assay, which tests long-term stem cell function in a controlled *in-vitro* environment (Miller *et al*, 2008). The initial cultures of 3000 *Mtg16*-null lineage-negative cells contained the same number of CFU-C-producing cells as 3000 wild-type lineage-negative cells. The same was true after 1 week in culture (Figure 5B). However, by the second week of culture, the number of CFU-C-producing cells present in the *Mtg16*-null cultures was drastically reduced compared with the wild-type cultures, and almost completely absent after just 3 weeks in culture (Figure 5B), suggesting a loss of self-renewal.

Mechanistically, Mtg16 can be recruited by many transcription factors that regulate stem cell function including Gfi1, TAL1/SCL, the 'E proteins' such as E2A, and mediators

©2012 European Molecular Biology Organization

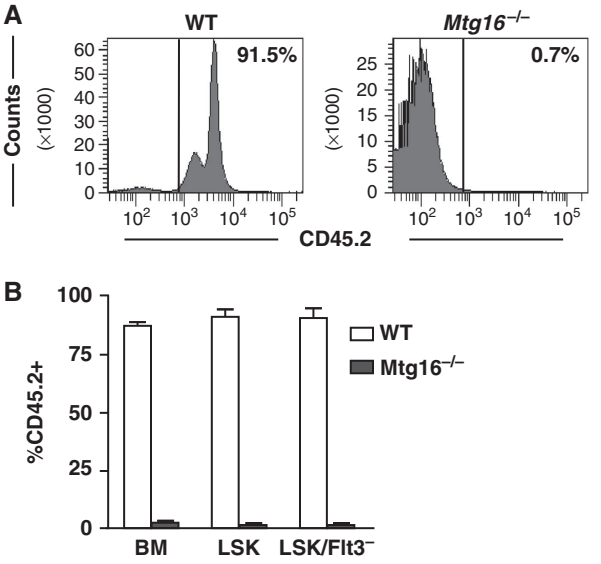

Figure 3 Serial transplantation reveals requirements for *Mtg16* in the maintenance of stem cells. (**A**) Flow cytometry analysis of whole bone marrow to determine the percentage of CD45.2 that had repopulated the bone marrow (BM) 6 weeks after secondary bone marrow transplantation from an initial competitive repopulation assay. A representative plot from an experiment performed in triplicate that is consistent with other biological replicates is shown. (**B**) Graphical representation of the quantification of CD45.2 cells residing in the BM and LSK or LSK/Flt3^{-} compartments 6 weeks after secondary BM transplantation.

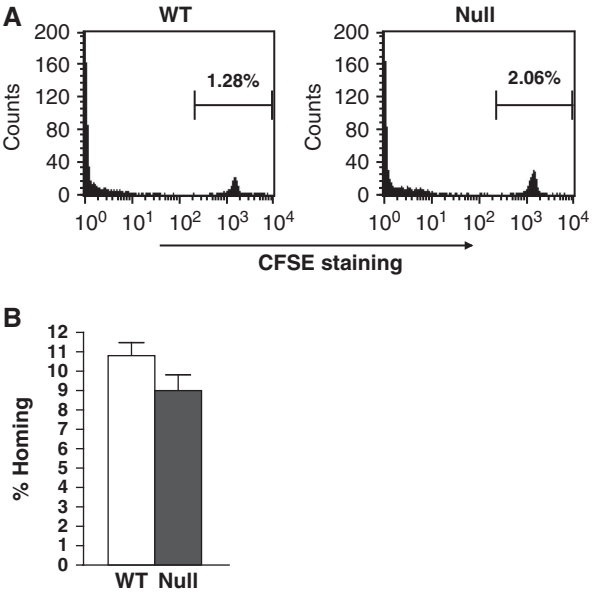

Figure 4 *Mtg16*$^{-/-}$ cells home to the bone marrow. (**A**) Bone marrow from control wild-type and *Mtg16*$^{-/-}$ mice was stained with CFSE and injected into lethally irradiated recipient mice. The bone marrow was analysed by flow cytometry to identify CFSE-labelled cells. (**B**) Representative graph of the number of colony-forming cells that homed to the bone marrow 16 h after injection into lethally irradiated recipient mice.

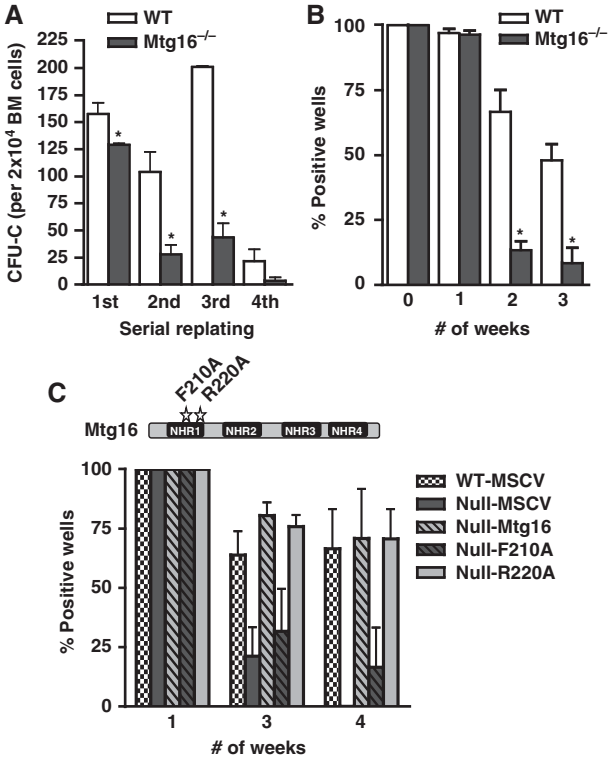

Figure 5 Inactivation of *Mtg16* impairs stem cell self-renewal. (**A**) Graphical representation of the numbers of methylcellulose colonies formed during serial replating assays where 2×10^4 cells were plated every 7 days for 4 weeks (wild type, empty bars; *Mtg16*-null, full bars). Data are expressed as mean ± s.e.m. An unpaired two-tailed *t*-test indicated these differences were statistically significant (marked by an *; first, $P = 0.03$; second, $P = 0.01$; third, $P < 0.001$; $n = 4$). Representative results from an experiment done in duplicate that are consistent with other biological replicates are shown. (**B**) Graphical representation of the numbers of methylcellulose colonies formed at the indicated times from LTC-IC cultures of wild-type (open bars) and *Mtg16*-null (full bars) bone marrow cells. Data are expressed as mean ± s.e.m. An unpaired two-tailed *t*-test indicated the difference at week 2 and week 3 after culture (marked with an *) was statistically significant ($P < 0.05$; $n = 4$). Representative results from three separate experiments are shown. (**C**) *Mtg16* re-expression, but not Mtg16-F210A, complements the LTC-IC defect in *Mtg16*-null bone marrow cells. Schematic diagram shows the positions of the F210A (blocks Mtg8 binding to HEB and Mtg16 suppression of E protein-dependent transcription) and R220A (control mutation that does not affect E protein binding in the crystal structure of Mtg8) point mutants.

of Wnt and Notch signalling (TCF4 and CSL) (Melnick *et al*, 2000; McGhee *et al*, 2003; Chevallier *et al*, 2004; Zhang *et al*, 2004; Schuh *et al*, 2005; Goardon *et al*, 2006; Moore *et al*, 2008; Salat *et al*, 2008; Engel *et al*, 2010). To begin to address which of these pathways might be critical to Mtg16-dependent stem cell functions, we re-expressed Mtg16, or a point mutant of Mtg16 that fails to suppress E protein-dependent transcription (F210A; R220A is a control mutation) (Hunt *et al*, 2011) in null BM cells and performed LTC-IC assays (Figure 5C; see Supplementary Figure S5 for expression controls). Wild-type Mtg16 and the R220A mutant complemented the LTC-IC defect, further suggesting that these defects were not due to the *in vivo* microenvironment. However, the F210A point mutant that disrupts one of the two contact sites for binding to E proteins (Plevin *et al*, 2006; Guo *et al*, 2009) only partially complemented this defect. Thus, E protein-dependent effects contribute to the *Mtg16*$^{-/-}$ phenotype.

 ©2012 European Molecular Biology Organization

The inactivation of Mtg16 alters the expression of cell-cycle control genes

Given that Mtg16 appears to act as a transcriptional co-repressor, we compared gene expression in control and *Mtg16*-null lineage-negative, Sca1$^+$, c-Kit$^+$ cells using cDNA microarray analysis. Because these cells are rare, LSK cells were sorted and pooled from 10 wild-type and 10 *Mtg16*-null mice and the experiment was performed using biological triplicates. We consistently observed changes in genes that function in haematopoietic differentiation, including, 4–6-fold higher levels of *Id1* and *Id2*, whose overexpression caused skewing of lineage allocation towards myelopoiesis and away from lymphopoiesis (Buitenhuis *et al*, 2005). The genes showing changes were categorized based on biological pathways or biological processes using the Panther classification system and genes that are associated with cell-cycle control, or the transition out of quiescence, were upregulated including *Fos*, *E2F2*, *Raf1*, *Cyclin D1*, *Cdk2*, and *N-Myc* (*P*-value of 0.05 for cell-cycle classification; representative cell-cycle control genes are shown in Figure 6A, see Supplementary Tables S1 and S2 for the lists of genes two-fold up or down) (Thomas *et al*, 2003). The microarray data were confirmed using selected genes whose expression was altered in the arrays, including *Id1*, *Id2*, and *E2F2* that were upregulated and the *Erythropoietin receptor* (*Epor*), which was dramatically downregulated (Figure 6B). The low level of *Epor* is important given the defects previously observed in 'stress' erythropoiesis in the absence of *Mtg16* (Chyla *et al*, 2008).

The levels of several key cell-cycle control genes were consistently 2–4-fold higher than in control cells in either microarray data or by QRT–PCR (Figure 6A and B). Therefore, we used ChIP assays to determine whether any of these genes are direct targets for regulation by Mtg16/Eto2. We focused the ChIP assays towards regions of these genes that are bound by factors that recruit MTG family members including TCF4, E proteins, and CSL or that were identified by overexpression of Mtg16 or Mtgr1 (Soler *et al*, 2010). While we were unable to detect Mtg16 at the TCF4, E protein, or CSL binding sites in the *Cyclin D1* or *N-Myc* promoters in MEL cells that express high levels of Mtg16 (Supplementary Figure S6), we detected Mtg16 near an E2A binding motif in the first intron of *E2F2* (Lin *et al*, 2010), which we confirmed using anti-E47 (Figure 6C). Mtg16/Eto2 localized to this site in *E2F2* using two sets of primers (Figure 6C) and two additional anti-Mtg16/ETO2 antibodies (Hunt, Engel, and Hiebert, unpublished data). While negative data with ChIP does not rule out the possibility that Mtg16 is required to suppress *Cyclin D1* or *N-Myc* or other regulators of the cell cycle, Mtg16 associates with *E2F2*, whose overexpression is sufficient to drive quiescent cells into the S phase (DeGregori *et al*, 1997).

Mtg16 is required for maintaining stem cell quiescence

The upregulation of cell-cycle control genes suggested that the exhaustion of stem cells after serial competitive transplant of *Mtg16*$^{-/-}$ BM could be due to inappropriate entry of the stem cell population into the cell cycle. To test this hypothesis, BrdU was injected into control and *Mtg16*$^{-/-}$ mice to assess the number of LSK cells in the S phase of the cell cycle. Two hours after injecting with BrdU, flow cytometric analysis revealed that a higher portion of LSK cells from *Mtg16*$^{-/-}$ mice incorporated BrdU, as compared with wild-type cells, indicating that more *Mtg16*-null stem and early progenitor cells had entered the cell cycle (Figure 7A; see Supplementary Figure S7A for further quantification). Further analysis of the cell cycle was performed by flow cytometry analysis of the incorporation of the DNA dye Hoechst 33342 (HO) and RNA dye Pyronin Y (PY), which identifies quiescent cells based on their lower output of RNA. The lower percentage of *Mtg16*$^{-/-}$ LSK cells that were Hoechst and Pyronin low (G_0 cells) compared with wild-type mice indicated a loss of quiescent cells (Figure 7B; see Supplementary Figure S7B for further quantification). Finally, we examined the LSK/Flt3$^-$ and the LSK/CD150$^+$/CD48$^-$ long-term HSC compartments and found that in the absence of *Mtg16*, nearly two third more LSK/Flt3$^-$ or LSK/CD150$^+$/CD48$^-$ cells incorporated BrdU indicating that these cells were in the cell cycle (Figure 7C and D; see Supplementary Figure S7C and D for FACS plots). These data suggest that loss of *Mtg16* allowed stem cell entry into the cell cycle.

Both the methylcellulose serial replating and LTC-IC assays suggest that the *Mtg16*-null stem/progenitor cells have decreased self-renewal potential and, together with the competitive BM transplants, suggest that Mtg16 may have intrinsic functions in the HSC. Therefore, we performed BrdU incorporation analysis on mice after competitive BM transplantation using 90% null cells and 10% wild type. Because the yield of *Mtg16*$^{-/-}$ cells is low after transplant (Figure 2), we were only able to examine LSK cells (rather than LSK/Flt3$^-$). Nevertheless, even in the presence of wild-type progenitor cells that negate any *Mtg16*$^{-/-}$ progenitor cell defects, the *Mtg16*$^{-/-}$ LSK population showed an increase in the percentage of cycling cells, as compared with the control mice containing wild-type CD45.2$^+$ LSK cells (Figure 7E). These results suggest that the increased cycling observed in the LSK compartment was not due to downstream defects in progenitor cells, but that *Mtg16/Eto2* is required to suppress stem cell entry into the cell cycle.

Discussion

In this study, we examined the role of *Mtg16*, a transcriptional co-repressor, in HSC functions. Inactivation of *Mtg16* reduced HSC numbers, and more importantly, resulted in a loss of self-renewal both *in vivo* and *in vitro*. This loss of self-renewal and eventual stem cell exhaustion appeared to be due to inappropriate entry of stem cells into the cell cycle. One function of Mtg16 is to link DNA binding transcription factors that control haematopoiesis to chromatin modifying enzymes such as histone deacetylases. We found that *E2F2*, a transcription factor that when overexpressed was sufficient to drive quiescent fibroblasts into the cell cycle, was upregulated in *Mtg16*$^{-/-}$ LSK cells. In addition, Mtg16 robustly associated with an enhancer-like sequence in the first intron of *E2F2*, suggesting that *E2F2* is a direct target for Mtg16-mediated repression. However, this does not preclude Mtg16-dependent regulation of other key regulators of the cell cycle. Notably, *N-Myc* was consistently overexpressed in gene expression analysis of *Mtg16*$^{-/-}$ cells (Chyla *et al*, 2008). Thus, Mtg16/Eto2 is likely required to maintain control of a cell-cycle regulatory circuit that when misregulated can drive quiescent stem cells into DNA synthesis or prevent cycling stem cells from entering G_0 (DeGregori *et al*, 1997).

©2012 European Molecular Biology Organization

A

Gene name	Gene symbol	Fold change
FBJ osteosarcoma oncogene	Fos	6.10
Glycogen synthase kinase 3 beta	Gsk3b	5.23
Sporulation protein, meiosis-specific, SP011 homologue (*S. cerevisiae*)	Spo11	4.69
Cyclin-dependent kinase 2	Cdk2	4.10
Cyclin G2	Ccng2	3.80
Janus kinase 2	Jak2	3.41
V-raf-leukaemia viral oncogene 1	Raf1	2.94
E2F transcription factor 2	E2F2	2.79
Cyclin D1	Ccnd1	2.70
Reticuloendotheliosis oncogene	Rel	2.68
CDC14 cell division cycle 14 homologue B (*S. cerevisiae*)	Cdc14b	2.50
CDC14 cell division cycle 14 homologue A (*S. cerevisiae*)	Cdc14a	2.11
Polo-like kinase 4 (*Drosophila*)	Plk4	1.71
Cell division cycle 25 homologue B (*S. cerevisiae*)	Cdc25b	1.60

Gene name	Gene symbol	Fold change
Retinoid X receptor alpha	Rxra	0.63
Polymerase (DNA directed), delta 1, catalytic subunit	Pold1	0.59
Polymerase (DNA directed), gamma	Polg	0.53
Lethal(3)malignant brain tumour-like 2 (*Drosophila*)	L3mbtl2	0.50
Cell division cycle 34 homologue (*S. cerevisiae*)	Cdc34	0.50
Checkpoint kinase 1 homologue (*S. pombe*)	Chek1	0.47
CDC23 (cell division cycle 23, yeast, homologue)	Cdc23	0.41
X-ray repair complementing defective repair in Chinese hamster cells 2	Xrcc2	0.38
Minichromosome Maintenance deficient 2 mitotin (*S. cerevisiae*)	Mcm2	0.38
Cyclin E1	Ccne1	0.37

B

	Mtg16-null versus WT	
	Microarray	RT–PCR
CcnD1	2.71 ± 0.23	2.25 ± 0.25
E2F2	2.39 ± 0.49	2.7 ± 0.1
GATA3	1.85 ± 0.03	2.0 ± 0.40
Gfi1	NC	0.125 ± 1.38
Id1	5.6 ± 2.54	4.85 ± 1.25
Id2	6.61 ± 0.65	5.15 ± 0.85
N-myc	2.6 ± 0.06	3.55 ± 0.45
EpoR	–5.04 ± 3.27	–16.65 ± 6.65

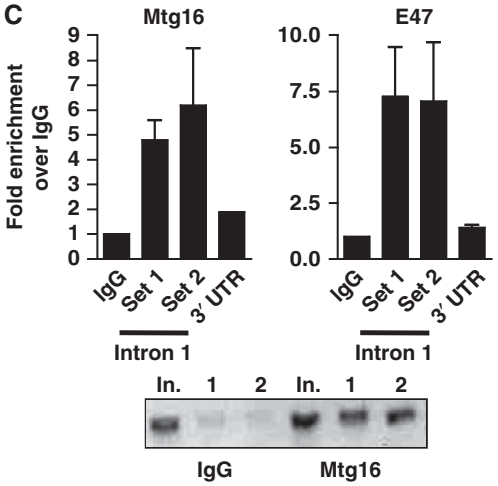

Figure 6 *Mtg16*-null LSK cells have altered gene expression patterns. (**A**) Gene expression profiling of mRNA from LSK cells isolated from wild-type and *Mtg16*-null mice was analysed using cDNA microarrays. Panther ontology analysis was used to group genes into specific biological processes and representative genes associated with cell-cycle control with their relative expression levels when *Mtg16* is deleted are shown. (**B**) Quantitative RT–PCR of selected genes was used to validate the microarray studies. (**C**) Mtg16 associates with the first intron of *E2F2*. Chromatin immunoprecipitated with the either control IgG or anti-Mtg16/Eto2 from lysates of MEL cells was amplified with two sets of primers (Set 1 and Set 2) that encompass an E2A binding site in the first intron of *E2F2*, or as a control, the 3′ untranslated region (UTR) of *E2F2* using quantitative PCR. Graph shows the level of signal relative to IgG set to '1'. The panel at the right shows ChIP using anti-E47 with the same *E2F2* first intron primers. The ethidium bromide-stained agarose gel shows a representative PCR stopped after 30 cycles; In., input; 1 and 2 designate the duplicate PCR samples from the ChIP reaction using primer set #2 flanking the E2A binding site.

The site in the *E2F2* gene that was selected for ChIP was based on ChIP-seq data linking E2A to this region (Lin *et al*, 2010) and we confirmed that E2A does associate with this sequence (Figure 6C), suggesting that E2A or other E proteins recruit Mtg16 to *E2F2* to control entry of cells into the cell cycle. The E proteins (e.g., E2A, E2-2, and HEB) belong to a family of helix-loop-helix transcription factors that activate transcription by binding to the 'E-box'. These factors contain two activation domains, and the most N-terminal activation domain is also a key contact point for MTG/ETO family members (Plevin *et al*, 2006; Guo *et al*, 2009; Park *et al*, 2009). The ability of E proteins to activate transcription is modulated by the Id proteins as well as by TAL1/SCL and related proteins. In proteomic analyses, MTG/ETO family members have been found in complexes containing E proteins, TAL1/SCL, Lmo2, Gfi1, GATA factors, other transcriptional co-repressors, and Tif1γ, which regulates transcriptional elongation (McGhee *et al*, 2003; Schuh *et al*, 2005; Hamlett *et al*, 2008; Cai *et al*, 2009; Bai *et al*, 2010; Fujiwara *et al*, 2010). While it is still unclear whether these proteomic studies are detecting one large complex or several smaller complexes, our results are consistent with *Mtg16* acting as a co-repressor, perhaps by binding to E2A, such that the inactivation of *Mtg16* caused increased expression of *E2F2*, as well as other cell-cycle control factors. It is notable that the phenotypes that arise in mice engineered to delete

 ©2012 European Molecular Biology Organization

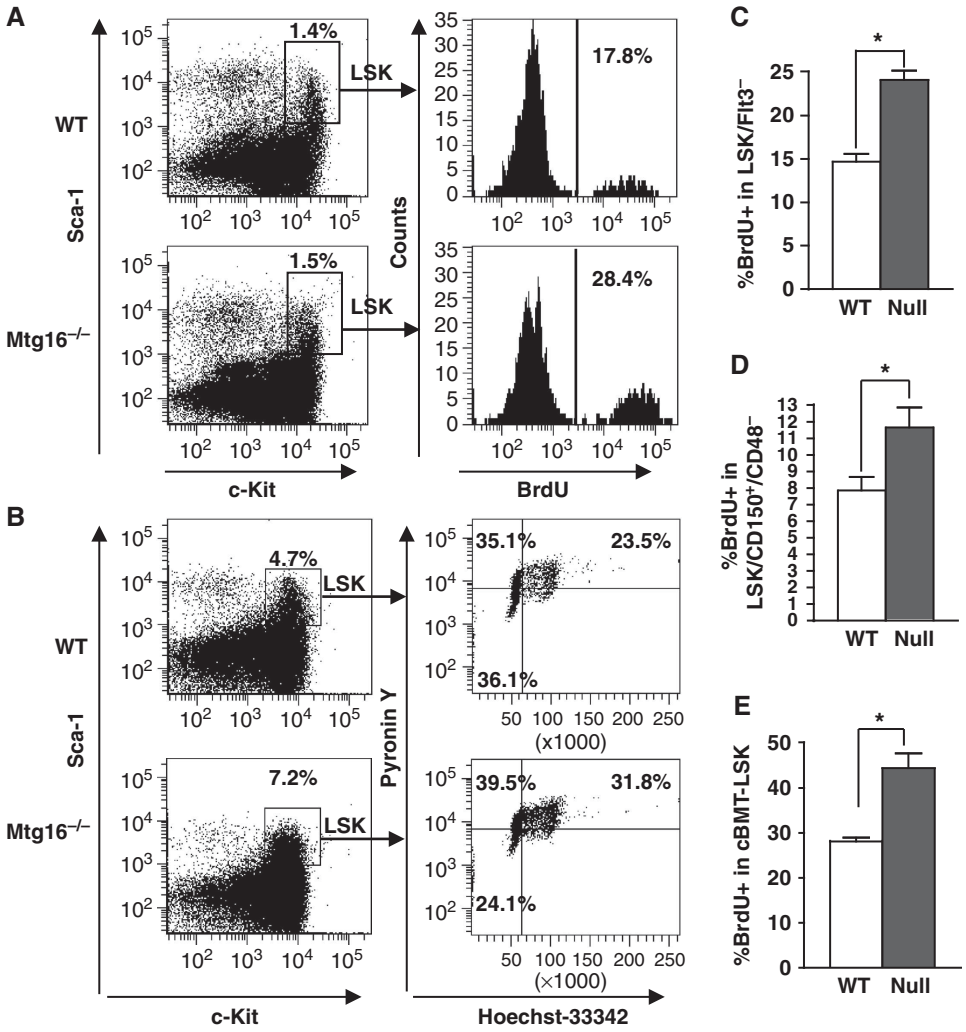

Figure 7 Inactivation of *Mtg16* leads to a decrease in the number of quiescent LSK cells. (**A**) Cell-cycle status of LSK cells was analysed using BrdU. A representative FACS plot from an experiment performed with five mice that is consistent with other biological replicates is shown. (**B**) Cell-cycle status of LSK cells was analysed with the DNA dye Hoechst 33342 (HO) and the RNA dye Pyronin Y (PY). A representative plot from an experiment performed in triplicate that is consistent with other biological replicates is shown. (**C**) Quantification of the percentage of LSK/Flt3$^-$ cells in S phase using BrdU incorporation as described in (**A**), but incorporating anti-Flt3. Data are expressed as mean ± s.e.m. and are consistent with other biological replicates. *An unpaired two-tailed *t*-test yielded $P<0.0001$; $n=6$. (**D**) Quantification of the percentage of LSK/CD150$^+$/CD48$^-$ cells in S phase using BrdU incorporation as described in (**A**). Data are expressed as mean ± s.e.m. and are consistent with other biological replicates. *An unpaired two-tailed *t*-test yielded $P=0.025$; wild type, $n=7$; *Mtg16*-null, $n=8$. (**E**) Quantification of the number of LSK cells in the S phase 5–6 weeks after competitive repopulation was analysed using BrdU as described in (**A**). Data are expressed as mean ± s.e.m. and are from biological replicates. *An unpaired two-tailed *t*-test yielded CD45.2 +, LSK BrdU +, $P=0.0069$; wild type, $n=4$; *Mtg16*-null, $n=8$.

E2A (Semerad *et al*, 2009) are similar to the defects found in the absence of *Mtg16* in regards to loss of HSC numbers and functions.

The defects we observed in *Mtg16*-null mice also closely resembled the phenotype associated with the deletion of *Lyl1*, a basic helix-loop-helix (bHLH) transcription factor that is closely related to TAL1/SCL and that may also associate with MTG/ETO family members (Capron *et al*, 2006; Bai *et al*, 2010). Although the *Lyl1*$^{-/-}$ mice displayed normal blood cell counts with only a slight reduction in the number of B cells, they too contain decreased numbers of LSK cells and LT-HSC frequencies, which resulted in decreased function in CFU-S_{12} and LTC-IC assays. In accordance, *Lyl-1*-null BM was severely impaired in its competitive repopulation abilities, especially in the ability to reconstitute the B and T cell lineages (Capron *et al*, 2006). However, the *Lyl1*-null BM did not recapitulate the increased propensity towards myeloid development that we observed in the absence of *Mtg16*. Given that Mtg16 is a co-repressor that interacts with multiple transcription factors and proteins, it is not surprising that its deletion would lead to more pleiotropic effects than the deletion of a single transcription factor. Taken together, these results highlight the importance of Mtg16 as a master regulator of haematopoiesis as it orchestrates the action of multiple transcription factors that are important for HSC functions in long-term self-renewal and in lineage cell fate decisions.

In addition to the involvement of Mtg16 in haematopoietic stem/progenitor cells, MTG family members may contribute to the function of other types of stem and progenitor cells. Mice with a deletion of *Mtgr1* failed to maintain secretory

©2012 European Molecular Biology Organization

lineage cells in the small intestine (Amann *et al*, 2005). After treatment with the ulcerative agent dextran sodium sulphate, which denudes the colonic epithelium, the *Mtgr1*-null colons displayed bifide glands and loss of glands, suggesting a defect in stem cell functions. These phenotypes were also associated with inappropriate cycling of the stem/progenitor cells in the crypts of the small intestine (Martinez *et al*, 2006). Gene targeting studies of *Mtg8* indicated that it is required for the development of the murine gut as some pups died due to deletion of the mid-gut (Calabi *et al*, 2001). In mice that retained the mid-gut, there was a dramatic loss of architecture, which could be due to defective stem cells. Thus, it is possible that all three MTG/ETO family members function in adult stem cells, perhaps to prevent entry into the cell cycle.

Our work may also hint of a role for MTG/ETO factors in leukaemogenesis. Although little has been done with the t(16;21), the t(8;21) is viewed as a relatively weak oncogene, as patients can carry this translocation for several years before developing AML (Peterson and Zhang, 2004). However, in mouse models of t(8;21) AML, the oligomerization domain, which also binds to endogenous Mtg16/Eto2 and Mtgr1, is essential to the transforming ability of the fusion protein (Yan *et al*, 2004, 2009). Therefore, it is possible that binding of the t(8;21) fusion protein to Mtg16 impairs the action of Mtg16 and causes the HSC to enter the cell cycle. In addition, the fusion protein can directly repress the expression of tumour suppressors such as $p14^{ARF}$, *Neurofibromatosis-1*, *PU.1*, and *C/EBPa* (Pabst *et al*, 2001; Linggi *et al*, 2002; Vangala *et al*, 2003; Yang *et al*, 2005). These data suggest that the t(8;21) could promote immortalization of haematopoietic stem and progenitor cells by repressing tumour suppressor genes, while triggering proliferation by activating genes such as *E2F2*.

Materials and methods

Mice

Mtg16-null mice were generated in our laboratory as previously described (Chyla *et al*, 2008) and backcrossed for up to 10 generations with C57BL6 mice purchased from NCI/Charles Rivers.

Cell culture and expression analysis

OP9-GFP stromal cells were cultured in α-MEM (Gibco) supplemented with 20% heat-inactivated fetal bovine serum (FBS), 50 U/ml penicillin, and 50 μg/ml streptomycin. Bosc23 cells were cultured in Dulbecco's modified Eagle Medium (DMEM) supplemented with 10% FBS, 50 U/ml penicillin, 50 μg/ml streptomycin, and 2 mM L-glutamine. Expression from MSCV-IRES-*GFP* plasmids was confirmed after transfection of 3 μg of plasmid into Bosc23 virus-producing cells with PolyFect (Qiagen). Plasmid construction was previously described (Hunt *et al*, 2011). At 48 h post transfection, cells were harvested into radioimmunoprecipitation assay (RIPA) buffer containing protease inhibitors, diluted 1:2 in Laemmli's sample buffer (Bio-Rad), sonicated, and subjected to 10% sodium dodecyl sulphate-polyacrylamide gel electrophoresis. Immunoblot analyses were performed using anti-Myc 9E10 antibody, with actin expression (Sigma) as a loading control. Expressed proteins were visualized using fluorophore-conjugated secondary antibodies and the Odyssey system (LiCor).

Flow cytometry analysis

Single cell suspensions were obtained by flushing the tibia and femur. Following treatment with erythrocyte lysis buffer, the remaining cells were stained with antibodies against: CD3, Ter119, Gr1, Mac1, B220, ScaI, c-Kit, CD45.1, CD45.2, Flt3, CD150, or CD48. Analysis was performed on a Becton Dickinson FACSCalibur or LSRII flow cytometer. To assess the cell-cycle status of the LSK cells, BM cells were resuspended in RPMI with 10% FBS and incubated with 10 μg/ml of Hoechst 33342 (Invitrogen) for 45 min at 37°C, washed and incubated with the indicated antibodies. Finally, the cells were fixed overnight at 4°C in 5% paraformaldehyde in PBS and incubated with 0.5 μM Pyronin Y (Polysciences, Inc.) for 30 min on ice prior to analysis. For the BrdU incorporation assays, mice were sacrificed 2 hours after intraperitoneal injection of 1 mg of BrdU. Cells were then harvested as previously described and labelled following the instructions of the BrdU Flow Kit (BD Pharmingen).

Microarray and real-time quantitative PCR

BM cells were harvested and the lineage-negative fraction was separated using the Lineage Cell Depletion Kit and MACS columns (Miltenyi Biotec). The lineage-negative fraction was then stained with antibodies for flow cytometry and the LSK cells were sorted on a Becton Dickinson FACSAria. Total RNA was extracted using the Versagene Total RNA Purification Kit (Gentra Systems) and microarray analysis was performed with the Applied Biosystem Inc. expression system. Probes with a signal-to-noise ratio of greater than 3 ranged from 43 to 50% of total probes. Quantile normalization was done using ABarray R script. Q-normalized data were put into GeneSpring to make comparisons. Probes without an SN greater than 3 in at least two of the five samples were excluded from the analysis. The microarray data were analysed using the Panther classification system for gene ontology classes based upon biological processes (Thomas *et al*, 2003). A *P*-value was calculated using the Mann–Whitney *U*-test (Wilcoxon Rank-Sum test) for each classification and the cell-cycle gene classification *P*-value using genes with at least 1.5-fold change was 0.006, and 0.05 using a two-fold change in null versus wild-type RNA. For the quantitative PCR, 1 μg of total RNA was transcribed with the iScript cDNA Synthesis kit (Bio-Rad) and 1/10 of the reaction was used for PCR using TaqMan primers on an automated ABI platform. PCRs were performed in triplicate. The expression of the gene of interest was calculated relative to the levels of *GusB*. Primer sequences were selected from the PrimerBank database (Wang and Seed, 2003). The gene expression of the MTG family members in the fibroblast cells was performed as previously described (Hunt *et al*, 2011).

Stem cell and progenitor cell assays

To perform the methylcellulose serial replating assays, we harvested BM and plated 2×10^4 total BM cells in methylcellulose media (Methocult GF M3434; Stem Cell Technologies). Every 7 days for 4 weeks, the numbers of colonies was counted, the plates were harvested, and 2×10^4 cells were replated in methylcellulose media. For the LTC-IC assay, 3×10^3 lineage-negative cells were cultured on OP9 stromal cells in a 96-well plate at 33°C and 5% CO_2 and weekly semi-replenishment of media (MyeloCultTM M5300 with 10^{-6} M hydrocortisone, Stem Cell Technologies) was performed (see Stem Cell Technologies website for a detailed protocol). At 1-week intervals, a set of wells was harvested and the cells were plated in methylcellulose media (Methocult GF M3434; Stem Cell Technologies) and cultured for 10 days to determine the percentage of positive wells (positive well scored with $\geqslant 1$ colony).

For Mtg16 re-expression in the LTC-IC assay, MSCV-*myc-Eto2-GFP* and variants (F210A and R220A) were transfected into Bosc23 virus-producing cells. The viral supernatant was collected at 48 h post transfection and filtered through a 45-μm syringe filter (Nalgene). Lineage-negative cells were centrifuged at 1500 r.p.m. for 1 h at room temperature with the viral supernatant prior to co-culture with OP9-GFP stromal cells and carried out as normal for the LTC-IC assay. Infection was monitored using flow cytometry to detect green fluorescent protein (GFP) expression from an aliquot of cells that were expanded for 5 days on OP9 stromal cells in RPMI supplemented with 10% heat-inactivated FBS, 50 U/ml penicillin, 50 μg/ml streptomycin, 5 ng/ml interleukin-6 (IL-6; Peprotech), 50 ng/ml stem cell factor (SCF; Peprotech) and 10^3 U/ml leukaemia inhibitory factor (LIF; Chemicon).

For BM transplantation, a single cell suspension of BM cells was obtained from the tibia and femur, and the red blood cells were lysed with erythrocyte lysis buffer (Buffer EL, Qiagen). BM cells were injected via the tail vein into lethally irradiated (900 rads) recipient wild-type C57Bl/6 mice. For competitive reconstitution assays, lethally irradiated C57Bl/6 CD45.1 congenic mice were used as recipients. The $Mtg16^{+/+}$ or *Mtg16*-null donor cells were mixed with C57Bl/6 CD45.1 BM cells (9:1). Reconstitution potential of the donor (CD45.2) cells was monitored by flow cytometry of the peripheral blood and BM. For the secondary competitive repopulation

 ©2012 European Molecular Biology Organization

transplants, the BM was harvested as described 12 weeks after the primary competitive transplant, and 2×10^6 total BM cells were injected into the tail vein of lethally irradiated recipients.

To assess total BM cell homing, we used the vital dye carboxyfluorescein succinimidyl ester (CFSE; Molecular Probes, Inc.), as previously described (Chyla *et al*, 2008). To assess progenitor cell homing, donor BM (WT or *Mtg16*-null) was harvested and prepared as described for the BM transplants. In all, 1×10^7 cells were injected via the tail vein into lethally irradiated recipient wild-type C57Bl/6 mice and an aliquot was also plated in methylcellulose culture to quantify the input number of committed progenitor cells. Sixteen hours later, the recipient mice were euthanized and the cells from the femur and tibia were harvested. Single-cell suspensions of the marrow cells were cultured in triplicate to assess the donor output colony-forming units in the recipient animals. For estimating total BM recovery, the femur/tibia content was assumed to represent 9% of total BM (Boggs, 1984).

ChIP assays

ChIP assays were performed using MEL cells. In all, 1×10^7 cells per condition were crosslinked with 1% formaldehyde (Sigma) for 20 min and the crosslinking reaction was quenched by the addition of glycine to a final concentration of 125 mM for 5 min. Cells were collected, washed, and resuspended in a low salt ChIP buffer (50 mM HEPES KOH, pH 7.5, 140 mM NaCl, 1 mM EDTA pH 8.0, 1% Triton X-100, and 0.1% Sodium Deoxycholate). Samples were sonicated and cleared by centrifugation, then precleared with the addition of Protein G Sepharose 4B (Sigma). Samples were incubated overnight with Goat IgG (Santa Cruz), anti-Eto2 G20 (Santa Cruz), anti-E47 SC-763x (Santa Cruz), or Rabbit IgG control (Millipore). Immune complexes were collected by incubation with Protein G Sepharose 4B (Sigma) then washed with a low salt ChIP buffer, a high salt ChIP buffer (50 mM HEPES KOH pH 7.5, 500 mM NaCl, 1 mM EDTA pH 8.0, 1% Triton X-100, and 0.1% Sodium Deoxycholate) and Lithium Chloride/NP-40 buffer (10 mM TrisCl, pH 8.0, 250 mM LiCl, 0.5% NP-40, 0.5% Sodium Deoxycholate). DNA–antibody complexes were eluted with elution buffer (1% SDS and 100 mM Sodium Bicarbonate) and the crosslink was reversed with 200 μM NaCl at 65°C. DNA was precipitated with the addition of 100% EtOH, RNase treated, Proteinase K (Sigma) treated, and isolated using the Qiagen PCR Purification kit. RT–PCR was performed with 2 μl of each sample in duplicate using SybrGreen (BioRad) and the BioRad ICycler and normalized to input. Primer sequences are as follows: E2F2 Intron 1: F-5′-GGACTCTGGAGGGCT AATGTTG-3′ R-5′-GCAATGTCTTCACTCGGCTCGG-3′; E2F2 Intron 2: F-5′TCAGACAGATGAGCGGGGAGGTG-3′ R-5′-GCCTCTGCCAGCCGC TTGAAA-3′; E2F2 3′ UTR F-5′-TGGTTTCCCCTCCCTGTGAGGC-3′ R-5′-AGACCTGTAGCCACCACGGTCC-3′; CCND1 TCF F-5′-CTGCCCGG CTTTGATCTCT-3′ R-5′-AGGACTTTGCAACTTCAACAAAACT-3′; CCND1 EBox/CSL F-5′-CTGGTCTGGCATCTTCGG-3′ R-5′-GAGAATGGGTGC GTTTCCG-3′; NMyc F-5′-CCCGAATGCCTACATAATTCT-3′ R-5′CCTT GGAAGGGTGGCTCA-3′; Mtg16 F-5′-AATATTCACAGGGCCTGACCA A-3′ R-5′-AAATGCCTGCAAGCGGATTA-3′.

Supplementary data

Supplementary data are available at *The EMBO Journal* Online (http://www.embojournal.org).

Acknowledgements

We thank the members of the Hiebert laboratory and Drs Christopher Klug (Univ. of Alabama, Birmingham) and David Williams (Children's Hospital Boston) for helpful discussions and encouragement. We thank the Vanderbilt CTSA (UL1 RR024975-01 from NCRR/NIH), Vanderbilt-Ingram Cancer Center (P30CA68485) and the Vanderbilt Digestive Diseases Research Center (5P30DK58404) for support and the use of shared resources including Flow Cytometry, the Vanderbilt Genome Sciences Resource, Transgenic/Embryonic Stem cell, and Human Tissue Acquisition and Pathology. This work was supported by National Institutes of Health (NIH) grants RO1-CA64140, RO1-CA112005, RO1-HL088494 (SWH), F30 HL093993 (AH), and Leukemia and Lymphoma Society postdoctoral fellowship #5074-03 (BJC).

Author contributions: MAF conceived and designed experiments, performed experiments, analysed data, and wrote the manuscript; IMM, AH, and BJC conceived and designed experiments, performed experiments, analysed data, and contributed to the writing of the manuscript; SWH conceived and designed experiments, analysed data, and wrote the manuscript with MAF.

Conflict of interest

The authors declare that they have no conflict of interest.

References

Amann JM, Chyla BJ, Ellis TC, Martinez A, Moore AC, Franklin JL, McGhee L, Meyers S, Ohm JE, Luce KS, Ouelette AJ, Washington MK, Thompson MA, King D, Gautam S, Coffey RJ, Whitehead RH, Hiebert SW (2005) Mtgr1 is a transcriptional corepressor that is required for maintenance of the secretory cell lineage in the small intestine. *Mol Cell Biol* **25:** 9576–9585

Amann JM, Nip J, Strom DK, Lutterbach B, Harada H, Lenny N, Downing JR, Meyers S, Hiebert SW (2001) ETO, a target of t(8;21) in acute leukemia, makes distinct contacts with multiple histone deacetylases and binds mSin3A through its oligomerization domain. *Mol Cell Biol* **21:** 6470–6483

Bai X, Kim J, Yang Z, Jurynec MJ, Akie TE, Lee J, LeBlanc J, Sessa A, Jiang H, DiBiase A, Zhou Y, Grunwald DJ, Lin S, Cantor AB, Orkin SH, Zon LI (2010) TIF1gamma controls erythroid cell fate by regulating transcription elongation. *Cell* **142:** 133–143

Boggs DR (1984) The total marrow mass of the mouse: a simplified method of measurement. *Am J Hematol* **16:** 277–286

Buitenhuis M, van Deutekom HW, Verhagen LP, Castor A, Jacobsen SE, Lammers JW, Koenderman L, Coffer PJ (2005) Differential regulation of granulopoiesis by the basic helix-loop-helix transcriptional inhibitors Id1 and Id2. *Blood* **105:** 4272–4281

Cai Y, Xu Z, Xie J, Ham AJ, Koury MJ, Hiebert SW, Brandt SJ (2009) Eto2/MTG16 and MTGR1 are heteromeric corepressors of the TAL1/SCL transcription factor in murine erythroid progenitors. *Biochem Biophys Res Commun* **390:** 295–301

Calabi F, Pannell R, Pavloska G (2001) Gene targeting reveals a crucial role for MTG8 in the gut. *Mol Cell Biol* **21:** 5658–5666

Capron C, Lecluse Y, Kaushik AL, Foudi A, Lacout C, Sekkai D, Godin I, Albagli O, Poullion I, Svinartchouk F, Schanze E, Vainchenker W, Sablitzky F, Bennaceur-Griscelli A, Dumenil D (2006) The SCL relative LYL-1 is required for fetal and adult hematopoietic stem cell function and B-cell differentiation. *Blood* **107:** 4678–4686

Chevallier N, Corcoran CM, Lennon C, Hyjek E, Chadburn A, Bardwell VJ, Licht JD, Melnick A (2004) ETO protein of t(8;21) AML is a corepressor for Bcl-6 B-cell lymphoma oncoprotein. *Blood* **103:** 1454–1463

Chyla BJ, Moreno-Miralles I, Steapleton MA, Thompson MA, Bhaskara S, Engel M, Hiebert SW (2008) Deletion of Mtg16, a target of t(16;21), alters hematopoietic progenitor cell proliferation and lineage allocation. *Mol Cell Biol* **28:** 6234–6247

Dalla-Favera R, Bregni M, Erikson J, Patterson D, Gallow RC, Croce CM (1982) Human c-myc onc gene is located on the region of chromosome 8 that is translocated in Burkitt lymphoma cells. *Proc Natl Acad Sci USA* **79:** 7824–7827

Davis JN, Williams BJ, Herron JT, Galiano FJ, Meyers S (1999) ETO-2, a new member of the ETO-family of nuclear proteins. *Oncogene* **18:** 1375–1383

DeGregori J, Leone G, Miron A, Jakoi L, Nevins JR (1997) Distinct roles for E2F proteins in cell growth control and apoptosis. *Proc Natl Acad Sci USA* **94:** 7245–7250

Deneault E, Cellot S, Faubert A, Laverdure JP, Frechette M, Chagraoui J, Mayotte N, Sauvageau M, Ting SB, Sauvageau G (2009) A functional screen to identify novel effectors of hematopoietic stem cell activity. *Cell* **137:** 369–379

Engel ME, Nguyen HN, Mariotti J, Hunt A, Hiebert SW (2010) Myeloid translocation gene 16 (MTG16) interacts with Notch transcription complex components to integrate Notch signaling

©2012 European Molecular Biology Organization

in hematopoietic cell fate specification. *Mol Cell Biol* **30:** 1852–1863

Erickson P, Gao J, Chang KS, Look T, Whisenant E, Raimondi S, Lasher R, Trujillo J, Rowley J, Drabkin H (1992) Identification of breakpoints in t(8;21) acute myelogenous leukemia and isolation of a fusion transcript, AML1/ETO, with similarity to Drosophila segmentation gene, runt. *Blood* **80:** 1825–1831

Fujiwara T, Lee HY, Sanalkumar R, Bresnick EH (2010) Building multifunctionality into a complex containing master regulators of hematopoiesis. *Proc Natl Acad Sci USA* **107:** 20429–20434

Gamou T, Kitamura E, Hosoda F, Shimizu K, Shinohara K, Hayashi Y, Nagase T, Yokoyama Y, Ohki M (1998) The partner gene of AML1 in t(16;21) myeloid malignancies is a novel member of the MTG8(ETO) family. *Blood* **91:** 4028–4037

Gelmetti V, Zhang J, Fanelli M, Minucci S, Pelicci PG, Lazar MA (1998) Aberrant recruitment of the nuclear receptor corepressor-histone deacetylase complex by the acute myeloid leukemia fusion partner ETO. *Mol Cell Biol* **18:** 7185–7191

Goardon N, Lambert JA, Rodriguez P, Nissaire P, Herblot S, Thibault P, Dumenil D, Strouboulis J, Romeo PH, Hoang T (2006) ETO2 coordinates cellular proliferation and differentiation during erythropoiesis. *EMBO J* **25:** 357–366

Graninger WB, Seto M, Boutain B, Goldman P, Korsmeyer SJ (1987) Expression of Bcl-2 and Bcl-2-Ig fusion transcripts in normal and neoplastic cells. *J Clin Invest* **80:** 1512–1515

Guo C, Hu Q, Yan C, Zhang J (2009) Multivalent binding of the ETO corepressor to E proteins facilitates dual repression controls targeting chromatin and the basal transcription machinery. *Mol Cell Biol* **29:** 2644–2657

Hamlett I, Draper J, Strouboulis J, Iborra F, Porcher C, Vyas P (2008) Characterization of megakaryocyte GATA1-interacting proteins: the corepressor ETO2 and GATA1 interact to regulate terminal megakaryocyte maturation. *Blood* **112:** 2738–2749

Hildebrand D, Tiefenbach J, Heinzel T, Grez M, Maurer AB (2001) Multiple regions of ETO cooperate in transcriptional repression. *J Biol Chem* **276:** 9889–9895

Hock H, Hamblen MJ, Rooke HM, Schindler JW, Saleque S, Fujiwara Y, Orkin SH (2004) Gfi-1 restricts proliferation and preserves functional integrity of haematopoietic stem cells. *Nature* **431:** 1002–1007

Hope KJ, Jin L, Dick JE (2003) Human acute myeloid leukemia stem cells. *Arch Med Res* **34:** 507–514

Hunt A, Fischer M, Engel ME, Hiebert SW (2011) Mtg16/Eto2 contributes to murine T-cell development. *Mol Cell Biol* **31:** 2544–2551

Kan Z, Jaiswal BS, Stinson J, Janakiraman V, Bhatt D, Stern HM, Yue P, Haverty PM, Bourgon R, Zheng J, Moorhead M, Chaudhuri S, Tomsho LP, Peters BA, Pujara K, Cordes S, Davis DP, Carlton VE, Yuan W, Li L *et al* (2010) Diverse somatic mutation patterns and pathway alterations in human cancers. *Nature* **466:** 869–873

Kiel MJ, Yilmaz OH, Iwashita T, Yilmaz OH, Terhorst C, Morrison SJ (2005) SLAM family receptors distinguish hematopoietic stem and progenitor cells and reveal endothelial niches for stem cells. *Cell* **121:** 1109–1121

Kitabayashi I, Ida K, Morohoshi F, Yokoyama A, Mitsuhashi N, Shimizu K, Nomura N, Hayashi Y, Ohki M (1998) The AML1-MTG8 leukemic fusion protein forms a complex with a novel member of the MTG8(ETO/CDR) family, MTGR1. *Mol Cell Biol* **18:** 846–858

Li QL, Ito K, Sakakura C, Fukamachi H, Inoue K, Chi XZ, Lee KY, Nomura S, Lee CW, Han SB, Kim HM, Kim WJ, Yamamoto H, Yamashita N, Yano T, Ikeda T, Itohara S, Inazawa J, Abe T, Hagiwara A *et al* (2002) Causal relationship between the loss of RUNX3 expression and gastric cancer. *Cell* **109:** 113–124

Lin YC, Jhunjhunwala S, Benner C, Heinz S, Welinder E, Mansson R, Sigvardsson M, Hagman J, Espinoza CA, Dutkowski J, Ideker T, Glass CK, Murre C (2010) A global network of transcription factors, involving E2A, EBF1 and Foxo1, that orchestrates B cell fate. *Nat Immunol* **11:** 635–643

Lindberg SR, Olsson A, Persson AM, Olsson I (2005) The Leukemia-associated ETO homologues are differently expressed during hematopoietic differentiation. *Exp Hematol* **33:** 189–198

Linggi B, Muller-Tidow C, van de Locht L, Hu M, Nip J, Serve H, Berdel WE, van der Reijden B, Quelle DE, Rowley JD, Cleveland J, Jansen JH, Pandolfi PP, Hiebert SW (2002) The t(8;21) fusion protein, AML1 ETO, specifically represses the transcription of the p14(ARF) tumor suppressor in acute myeloid leukemia. *Nat Med* **8:** 743–750

Liu Y, Cheney MD, Gaudet JJ, Chruszcz M, Lukasik SM, Sugiyama D, Lary J, Cole J, Dauter Z, Minor W, Speck NA, Bushweller JH (2006) The tetramer structure of the Nervy homology two domain, NHR2, is critical for AML1/ETO's activity. *Cancer Cell* **9:** 249–260

Lutterbach B, Westendorf JJ, Linggi B, Patten A, Moniwa M, Davie JR, Huynh KD, Bardwell VJ, Lavinsky RM, Rosenfeld MG, Glass C, Seto E, Hiebert SW (1998) ETO, a target of t(8;21) in acute leukemia, interacts with the N-CoR and mSin3 corepressors. *Mol Cell Biol* **18:** 7176–7184

Martinez JA, Williams CS, Amann JM, Ellis TC, Moreno-Miralles I, Washington MK, Gregoli P, Hiebert SW (2006) Deletion of Mtgr1 sensitizes the colonic epithelium to dextran sodium sulfate-induced colitis. *Gastroenterology* **131:** 579–588

McGhee L, Bryan J, Elliott L, Grimes HL, Kazanjian A, Davis JN, Meyers S (2003) Gfi-1 attaches to the nuclear matrix, associates with ETO (MTG8) and histone deacetylase proteins, and represses transcription using a TSA-sensitive mechanism. *J Cell Biochem* **89:** 1005–1018

Melnick AM, Westendorf JJ, Polinger A, Carlile GW, Arai S, Ball HJ, Lutterbach B, Hiebert SW, Licht JD (2000) The ETO protein disrupted in t(8;21)-associated acute myeloid leukemia is a corepressor for the promyelocytic leukemia zinc finger protein. *Mol Cell Biol* **20:** 2075–2086

Miller CL, Dykstra B, Eaves CJ (2008) Characterization of mouse hematopoietic stem and progenitor cells. *Curr Protoc Immunol* **Chapter 22**, Unit 22B 22

Miyoshi H, Kozu T, Shimizu K, Enomoto K, Maseki N, Kaneko Y, Kamada N, Ohki M (1993) The t(8;21) translocation in acute myeloid leukemia results in production of an AML1-MTG8 fusion transcript. *EMBO J* **12:** 2715–2721

Miyoshi H, Shimizu K, Kozu T, Maseki N, Kaneko Y, Ohki M (1991) t(8;21) breakpoints on chromosome 21 in acute myeloid leukemia are clustered within a limited region of a single gene, AML1. *Proc Natl Acad Sci USA* **88:** 10431–10434

Moore AC, Amann JM, Williams CS, Tahinci E, Farmer TE, Martinez JA, Yang G, Luce KS, Lee E, Hiebert SW (2008) Myeloid translocation gene family members associate with T-cell factors (TCFs) and influence TCF-dependent transcription. *Mol Cell Biol* **28:** 977–987

Pabst T, Mueller BU, Harakawa N, Schoch C, Haferlach T, Behre G, Hiddemann W, Zhang DE, Tenen DG (2001) AML1-ETO down-regulates the granulocytic differentiation factor C/EBPalpha in t(8;21) myeloid leukemia. *Nat Med* **7:** 444–451

Park S, Chen W, Cierpicki T, Tonelli M, Cai X, Speck NA, Bushweller JH (2009) Structure of the AML1-ETO eTAFH domain-HEB peptide complex and its contribution to AML1-ETO activity. *Blood* **113:** 3558–3567

Peterson LF, Zhang DE (2004) The 8;21 translocation in leukemogenesis. *Oncogene* **23:** 4255–4262

Plevin MJ, Zhang J, Guo C, Roeder RG, Ikura M (2006) The acute myeloid leukemia fusion protein AML1-ETO targets E proteins via a paired amphipathic helix-like TBP-associated factor homology domain. *Proc Natl Acad Sci USA* **103:** 10242–10247

Salat D, Liefke R, Wiedenmann J, Borggrefe T, Oswald F (2008) ETO, but not leukemogenic fusion protein AML1/ETO, augments RBP-Jkappa/SHARP-mediated repression of notch target genes. *Mol Cell Biol* **28:** 3502–3512

Santaguida M, Schepers K, King B, Sabnis AJ, Forsberg EC, Attema JL, Braun BS, Passegue E (2009) JunB protects against myeloid malignancies by limiting hematopoietic stem cell proliferation and differentiation without affecting self-renewal. *Cancer Cell* **15:** 341–352

Schuh AH, Tipping AJ, Clark AJ, Hamlett I, Guyot B, Iborra FJ, Rodriguez P, Strouboulis J, Enver T, Vyas P, Porcher C (2005) ETO-2 associates with SCL in erythroid cells and megakaryocytes and provides repressor functions in erythropoiesis. *Mol Cell Biol* **25:** 10235–10250

Semerad CL, Mercer EM, Inlay MA, Weissman IL, Murre C (2009) E2A proteins maintain the hematopoietic stem cell pool and promote the maturation of myelolymphoid and myeloerythroid progenitors. *Proc Natl Acad Sci USA* **106:** 1930–1935

Shizuru JA, Negrin RS, Weissman IL (2005) Hematopoietic stem and progenitor cells: clinical and preclinical regeneration of the hematolymphoid system. *Annu Rev Med* **56:** 509–538

 ©2012 European Molecular Biology Organization

Silva FP, Morolli B, Storlazzi CT, Anelli L, Wessels H, Bezrookove V, Kluin-Nelemans HC, Giphart-Gassler M (2003) Identification of RUNX1/AML1 as a classical tumor suppressor gene. *Oncogene* **22:** 538–547

Soler E, Andrieu-Soler C, de Boer E, Bryne JC, Thongjuea S, Stadhouders R, Palstra RJ, Stevens M, Kockx C, van Ijcken W, Hou J, Steinhoff C, Rijkers E, Lenhard B, Grosveld F (2010) The genome-wide dynamics of the binding of Ldb1 complexes during erythroid differentiation. *Genes Dev* **24:** 277–289

Song WJ, Sullivan MG, Legare RD, Hutchings S, Tan X, Kufrin D, Ratajczak J, Resende IC, Haworth C, Hock R, Loh M, Felix C, Roy DC, Busque L, Kurnit D, Willman C, Gewirtz AM, Speck NA, Bushweller JH, Li FP *et al* (1999) Haploinsufficiency of CBFA2 causes familial thrombocytopenia with propensity to develop acute myelogenous leukaemia. *Nat Genet* **23:** 166–175

Thomas PD, Campbell MJ, Kejariwal A, Mi H, Karlak B, Daverman R, Diemer K, Muruganujan A, Narechania A (2003) PANTHER: a library of protein families and subfamilies indexed by function. *Genome Res* **13:** 2129–2141

Vangala RK, Heiss-Neumann MS, Rangatia JS, Singh SM, Schoch C, Tenen DG, Hiddemann W, Behre G (2003) The myeloid master regulator transcription factor PU.1 is inactivated by AML1-ETO in t(8;21) myeloid leukemia. *Blood* **101:** 270–277

Wang J, Hoshino T, Redner RL, Kajigaya S, Liu JM (1998) ETO, fusion partner in t(8;21) acute myeloid leukemia, represses transcription by interaction with the human N-CoR/mSin3/HDAC1 complex. *Proc Natl Acad Sci USA* **95:** 10860–10865

Wang X, Seed B (2003) A PCR primer bank for quantitative gene expression analysis. *Nucleic Acids Res* **31:** e154

Wood LD, Parsons DW, Jones S, Lin J, Sjoblom T, Leary RJ, Shen D, Boca SM, Barber T, Ptak J, Silliman N, Szabo S, Dezso Z, Ustyanksky V, Nikolskaya T, Nikolsky Y, Karchin R, Wilson PA, Kaminker JS, Zhang Z *et al* (2007) The genomic landscapes of human breast and colorectal cancers. *Science* **318:** 1108–1113

Yan M, Ahn EY, Hiebert SW, Zhang DE (2009) RUNX1/AML1 DNA-binding domain and ETO/MTG8 NHR2-dimerization domain are critical to AML1-ETO9a leukemogenesis. *Blood* **113:** 883–886

Yan M, Burel SA, Peterson LF, Kanbe E, Iwasaki H, Boyapati A, Hines R, Akashi K, Zhang DE (2004) Deletion of an AML1-ETO C-terminal NcoR/SMRT-interacting region strongly induces leukemia development. *Proc Natl Acad Sci USA* **101:** 17186–17191

Yang G, Khalaf W, van de Locht L, Jansen JH, Gao M, Thompson MA, van der Reijden BA, Gutmann DH, Delwel R, Clapp DW, Hiebert SW (2005) Transcriptional repression of the neurofibromatosis-1 tumor suppressor by the t(8;21) fusion protein. *Mol Cell Biol* **25:** 5869–5879

Zeng H, Yucel R, Kosan C, Klein-Hitpass L, Moroy T (2004) Transcription factor Gfi1 regulates self-renewal and engraftment of hematopoietic stem cells. *EMBO J* **23:** 4116–4125

Zhang J, Kalkum M, Yamamura S, Chait BT, Roeder RG (2004) E protein silencing by the leukemogenic AML1-ETO fusion protein. *Science* **305:** 1286–1289

©2012 European Molecular Biology Organization